Advances in Geo-Energy Research

Vol. 10, No. 1, p. 56-64, 2023

Original article

Impact of stress dependence of elastic moduli and poroelastic constants on earth surface uplift due to injection

Samin Raziperchikolaee*

Battelle Memorial Institute, Columbus, OH 43201, USA

Keywords:
Earth surface uplift
geomechanics
Biot coefficient
stress dependent elastic moduli
CO_2 sequestration

Cited as:
Raziperchikolaee, S. Impact of stress dependence of elastic moduli and poroelastic constants on earth surface uplift due to injection. Advances in Geo-Energy Research, 2023, 10(1): 56-64. https://doi.org/10.46690/ager.2023.10.06

Abstract:
Hydromechanical models have typically assumed constant stress-independent elastic moduli to estimate, forecast, and history-match earth surface uplift. The effect of stress-dependent elastic moduli and poroelastic constant (i.e., Biot coefficient) on Earth surface uplift during injection is investigated in this study. Experimental data gathered for different rock types shows that Biot coefficient and bulk modulus vary in response to Terzaghi effective stress. Stress-dependent elastic modulus was imported to the numerical model representing Berea sandstone. Hydromechanical simulations were performed to model CO_2 injection into the Berea reservoir by incorporating elastic moduli stress dependency. Hydromechanical modeling results show that using stress-independent elastic moduli causes under-estimation of Earth surface uplift due to injection. A decrease in Young's modulus and an increase in Biot coefficient because of injection can contribute to a higher estimated uplift. Neglecting the stress dependency effect could cause an erroneous estimate of potential surface uplift due to injection. The impact of geological properties of Berea and injecting brine instead of CO_2 on surface uplift trend were also investigated.

1. Introduction

Fluid injection into geological formations has been used for different purposes. Brine disposal, geological CO_2 sequestration, and nuclear waste disposal are examples of injection processes with no subsequent fluid production (Liu and Rutqvist, 2013; Zhang et al., 2022, 2023). Shale hydraulic fracturing using water-based fracturing fluid produces a large volume of flow-back brine. Brine injection into deep aquifers has been widely used to dispose produced brine (Sminchak, 2015). Geological CO_2 sequestration would be an approach to decrease the amount of emitted greenhouse gases into the atmosphere (Gale, 2004; Raziperchikolaee et al., 2013; Song et al., 2023). CO_2 has been recently injected in megatonne-scale at different sites around the world including Sleipner, Norway; Weyburn, Canada; and In-Salah, Algeria (Verdon et al., 2013; Furre et al., 2017; Raziperchikolaee and Pasumarti, 2020b). Other injection processes (e.g., injection into geothermal systems, waterflooding into the depleted reservoir, and enhanced oil recovery methods) have also been widely performed with simultaneous or subsequent production from target formations (Asghari et al., 2007; Alvarado and Manrique, 2010; Raziperchikolaee et al., 2020).

Earth surface uplift is among the risks associated with injection into geological formations (Raziperchikolaee et al., 2021). Interferometric Synthetic Aperture Radar (geomechanics) data analysis has indicated significant surface uplift (15-20 mm) above the injection wells over five years of injection at the In-Salah injection site (Bohloli et al., 2018; Jun et al., 2023). Northern Alberta oil production through enhanced oil recovery methods (Pearse et al., 2014), wastewater injection into a disposal well in West Texas (Zheng et al., 2019), gas storage in Lombardi field, Italy (Gambolati et al., 2000; Teatini et al., 2011; Gambolati and Teatini, 2015) are among the examples experiencing Earth surface uplift over the sites (detected using geomechanics).

Hydromechanical modeling (e.g., numerical, analytical, statistical based model) can be applied to assess the possibility of geomechanical risks including Earth surface uplift (Vidal-Gilbert et al., 2010; Rutqvist et al., 2016; Verdon and

Yandy Scientific Press

*Corresponding author.
E-mail address: raziperchikolae@battelle.org (R. Samin).

Received July 28, 2023; revised September 5, 2023; accepted September 27, 2023; available online October 1, 2023.

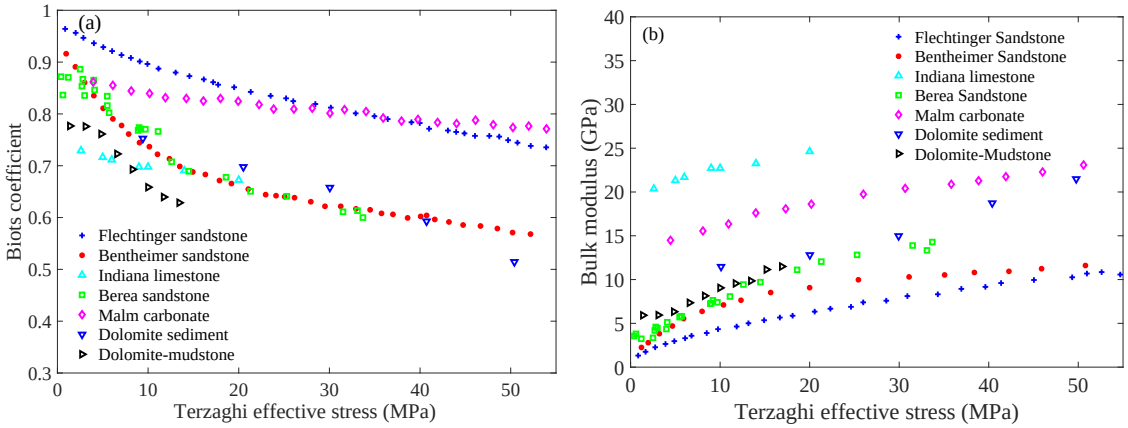

Fig. 1. (a) Biot coefficient of different rock types as a function of Terzaghi effective stress and (b) Bulk modulus of different rock types as a function of Terzaghi effective stress.

Stork, 2016). Multiphase flow-mechanical numerical models have been performed to predict expected uplift depending on the reservoir depth, type, and overburden formations' mechanical properties and interpret uplift measured by monitoring methods. Significant surface uplift observed at the In-Salah site has been explained through modeling of a conductive zone at the reservoir-caprock boundary using hydromechanical simulations (Bissell et al., 2011; Morris et al., 2011; Rinaldi et al., 2017). Numerical modeling of wastewater injection into a well in West Texas indicated that the brine leakage through casing cement could explain the observed uplift (16 cm) above the well (Zheng et al., 2019). Results of the hydromechanical modeling of enhanced oil recovery in northern Alberta showed that stress changes in the reservoir induced surface heave (varied from 4 to 18 cm at different sites) measured by geomechanics (Pearse et al., 2014).

Elastic moduli (i.e., Young's modulus, Poisson's ratio, bulk modulus, shear modulus) and poroelastic constant (i.e., Biot coefficient) of the reservoir are constant inputs in the hydromechanical modeling to estimate, forecast and history-match Earth surface uplift (Bjørnarå et al., 2018; Zheng et al., 2019; Raziperchikolaee and Pasumarti, 2020b) as well as other aspects of poroelastic responses including reservoir's stress path estimation (Vidal-Gilbert et al., 2010; Li and Laloui, 2016; Raziperchikolaee et al., 2019), fault activation prediction (Mazzoldi et al., 2012; Jha and Juanes, 2014; van et al., 2019), and induced seismicity (Raziperchikolaee and Miller, 2015). In this work, the changes in Biot coefficient and elastic moduli as a function of pore pressure and stress were reviewed using available experimental measurements for different rock types. As mentioned, Elastic moduli and Biot coefficient are typically assumed constant in the hydromechanical models. In this work, Elastic moduli were related to effective stress using linear and quadratic regressions for Berea sandstone and included in the numerical model. Hydromechanical modeling was then performed to investigate the potential effect of elastic moduli and Biot coefficient changes on surface uplift due to CO_2 injection into a Berea sandstone reservoir.

Rock physics experiments have been performed to measure Biot coefficient and elastic moduli values as a result of stress and pore pressure changes. Biot coefficient (α) is defined as the ratio of the fluid volume change divided by the change in bulk volume under the constraint that pore pressure remains constant (Wang, 2017). Direct and indirect methods have been applied to estimate Biot coefficient (Biot and Willis, 1957; Blöcher et al., 2014; Wang, 2017). Fig. 1 shows the Biot coefficient and bulk modulus changes as a function of Terzaghi effective stress for different rock types including sandstone (Warpinski and Teufel, 1992; Hart and Wang, 2010), carbonate (Hart and Wang, 2010; Hassanzadegan et al., 2016; Pei et al., 2018), and shale (Ma and Zoback, 2017). Terzaghi effective stress (σ') defines as:

$$\sigma' = \sigma - P \tag{1}$$

where σ is total stress and P is pore pressure. Figs. 1(a) and 1(b) show that Biot coefficient decreases, and bulk modulus increases as a result of Terzaghi effective stress increase in all rock types. Both the elastic moduli and Biot coefficient are strong functions of pore pressure and stress. Note that the trend of changes in elastic moduli and Biot coefficient would vary depending on pore structure, organic content, clay mineral, and microcracks presence (Warpinski and Teufel, 1992; Ma and Zoback, 2017; Li et al., 2020; Qin et al., 2022).

Changes in Biot coefficient and elastic moduli as a consequence of effective stress changes were investigated specifically for Berea sandstone in detail. The Biot coefficient and elastic moduli were measured for three Berea sandstone samples using different types of experimental measurement (i.e., unjacketed, drained, and undrained measurements) at various Terzaghi effective stresses (Hart, 2000; Hart and Wang, 2010). Note that additional experiments were performed to measure the bulk and grain compressibilities and estimate Biot coefficient indirectly. Results of additional tests (performed under additional pressure and stress) were added to Fig. 2(a) and used to achieve more accurate regression.

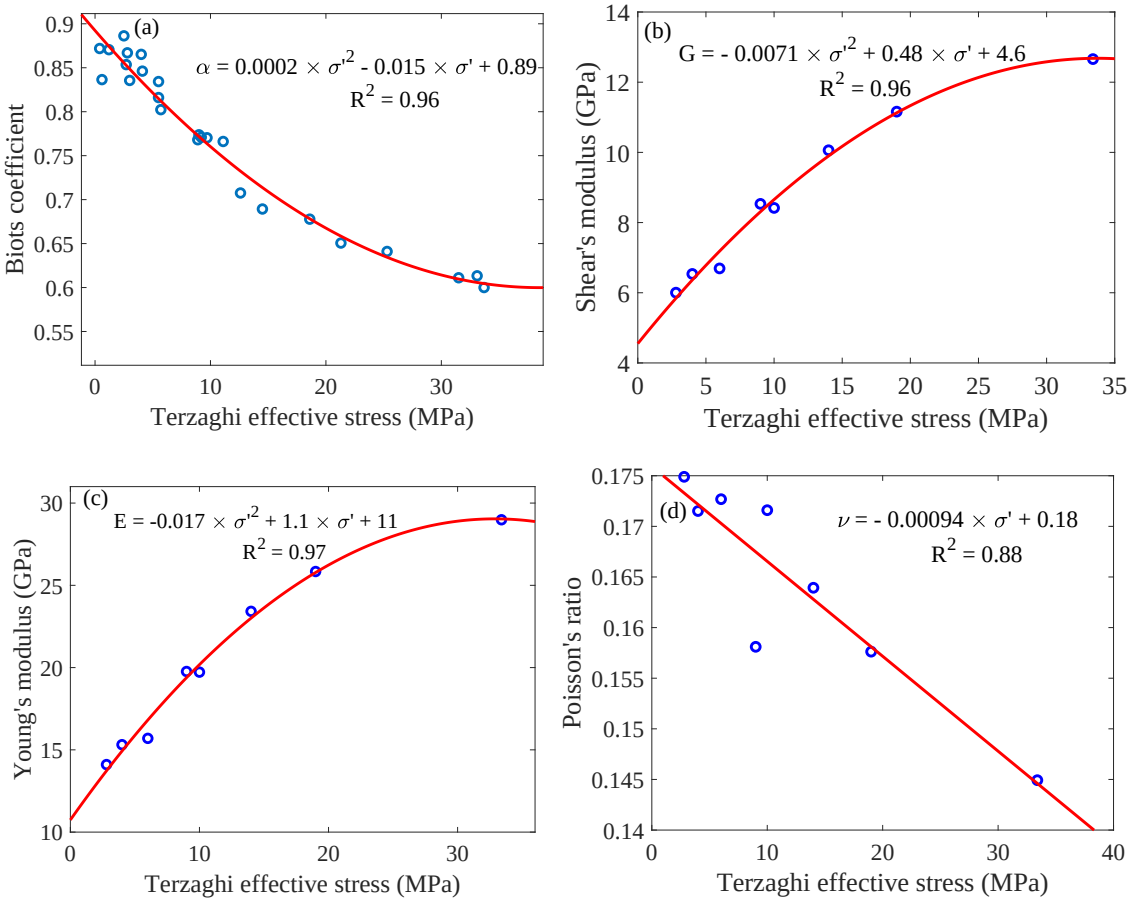

Fig. 2. (a) Biot coefficient (R^2 = 0.96), (b) Shear modulus (R^2 = 0.98), (c) Young's modulus (R^2 = 0.98), and (d) Poisson's ratio (R^2 = 0.83) as a function of effective stress. Note that additional experiments (under different pressure and stress (reflected in Fig. 2(a)) were used to estimate Biot coefficient.

2. Previous experimental investigation

Measured elastic moduli and Biot coefficient of Berea sandstone as a function of Terzaghi effective stress are shown in Fig. 2. Nonlinear elastic behavior of elastic moduli with respect to Terzaghi effective stress is observed in Berea sandstone at low effective stresses. Figs. 2(a)-2(c) show that the Berea samples tend to show more linear elastic behavior at higher effective stress then lower effective stress (specifically for Biot coefficient). The nonlinearity in elastic behavior at low effective stress is mainly due to the impact of microfractures and cracks. At low effective stress, microcracks are still open and contribute to the elastic behavior of the rock. However, at higher effective stress, rock is less compliant, microcracks are closed and donot contribute to the elastic behavior of the rock. As a result, the rock's elastic behavior is more linear (Hart, 2000; Hart and Wang, 2010). Quadratic regression was used to model effective stress dependency of Biot coefficient, Young's modulus, and shear modulus (Eqs. (2)-(4)). Linear regression was used to correlate Poisson's ratio and Terzaghi effective stress (Eq. (5)). R-squared is used to measure the accuracy of the model estimations. High R-squared shows a reliable correlation between elastic moduli and effective stress. The regression-based models were then imported into the numerical model to investigate the effect of stress dependency of elastic moduli and Biot coefficient on the poroelastic response to injection:

$$\alpha = 0.0002 \times \sigma'^2 - 0.015 \times \sigma' + 0.89 \quad (2)$$

$$G = -0.0071 \times \sigma'^2 + 0.48 \times \sigma' + 4.6 \quad (3)$$

$$E = -0.017 \times \sigma'^2 + 1.1 \times \sigma' + 11 \quad (4)$$

$$\upsilon = -0.00094 \times \sigma' + 0.18 \quad (5)$$

where α is Biot coefficient, G is shear modulus, E is Young's modulus, and υ is poisson's ratio.

3. Modeling investigation

Berea sandstone is one of the target formations for brine disposal in the Appalachian basin (Sminchak, 2015). In addition, accumulated oil in the Berea sandstone reservoir has been produced historically from different oil fields across the Appalachian basin (e.g., Chatham oil field, Clay oil field, Griffithsville field) (Riley et al., 2010). As a result, Berea sandstone is also a candidate for CO_2 storage and enhanced

Table 1. Hydromechanical model parameters.

Parameters	Values
Size of model	18,500 m × 18,500 m × 1,515 m
Number of grids	71 × 71 × 11
Reservoir top	1,500 m
Property variability	Varies by layer
Porosity (Reservoir, Caprock)	(0.01, 0.08)
Permeability (Reservoir, Caprock)	(0.0001, 10) mD
Model temperature	42 °C
Model initial pore pressure	15.5 MPa
Wellbore condition	Bottom hole pressure constraint
Injection period	30 years
Reservoir stress gradient	22, 22.6, 23.3 MPa/Km
Reservoir stress (minimum horizontal, maximum horizontal, vertical stress)	33, 34, 35 MPa
Young modulus of caprock	11 GPa
Poisson's ratio of caprock	0.2
Young modulus of reservoir (Model Scenario 1)	25 GPa
Poisson's ratio of reservoir (Model Scenario 1)	0.156
Biot coefficient (Model Scenario 1)	0.647

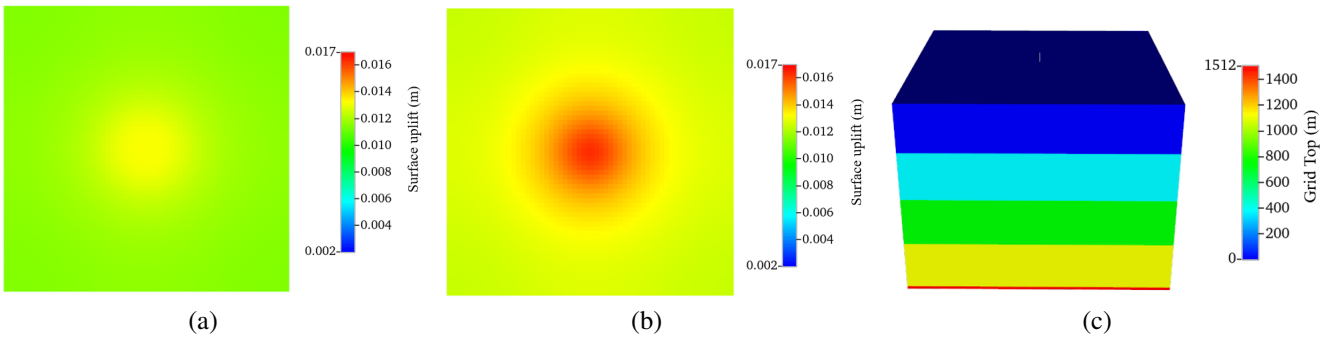

Fig. 3. (a) 3D schematic of the reservoir, (b) map view of Earth surface uplift with constant mechanical parameters and Biot coefficient (Model Scenario 1), and (c) map view of Earth surface uplift with modeling mechanical parameters and Biot coefficient stress-pressure dependency (Model Scenario 2).

oil recovery.

A 3D (three-dimensional) hydromechanical model was built to simulate CO_2 injection into the Berea sandstone aquifer and study the effect of stress dependency of elastic moduli on expected uplift. CMG-GEM was used to model the multiphase flow behavior of CO_2 injection into an aquifer fully saturated with brine (CMG-GEM, 2016). The geomechanics solver in CMG-GEM solves the mechanical equilibrium equations using finite element method. Using iterative coupling approach, the stress and strain are calculated in the model domain at each time step (Tran et al., 2004, 2010). The geological and fluid flow parameters in the model (thickness, depth, permeability, porosity) were assigned using available data for Berea sandstone (Sminchak, 2015). A well is placed in the center of the modeling grid to simulate the injection scenario. The model has a sealed outer boundary. A schematic of 3D model (color-coded by depth) is shown in Fig. 3. Van Genuchten equations were used to represent the relative permeability of CO_2-water system with the exponent of 0.457 (Van, 1980). The model was constrained using bottomhole pressure of 50 MPa. Cumulative CO_2 injection was estimated to be 10 million metric tons (5.4×10^9 cubic meters at standard condition) after 30 years of injection with an average rate of 333,000 metric tons per year as a result of numerical simulation. Table 1 shows the reservoir and geomechanical properties to build the model. Two modeling scenarios include:

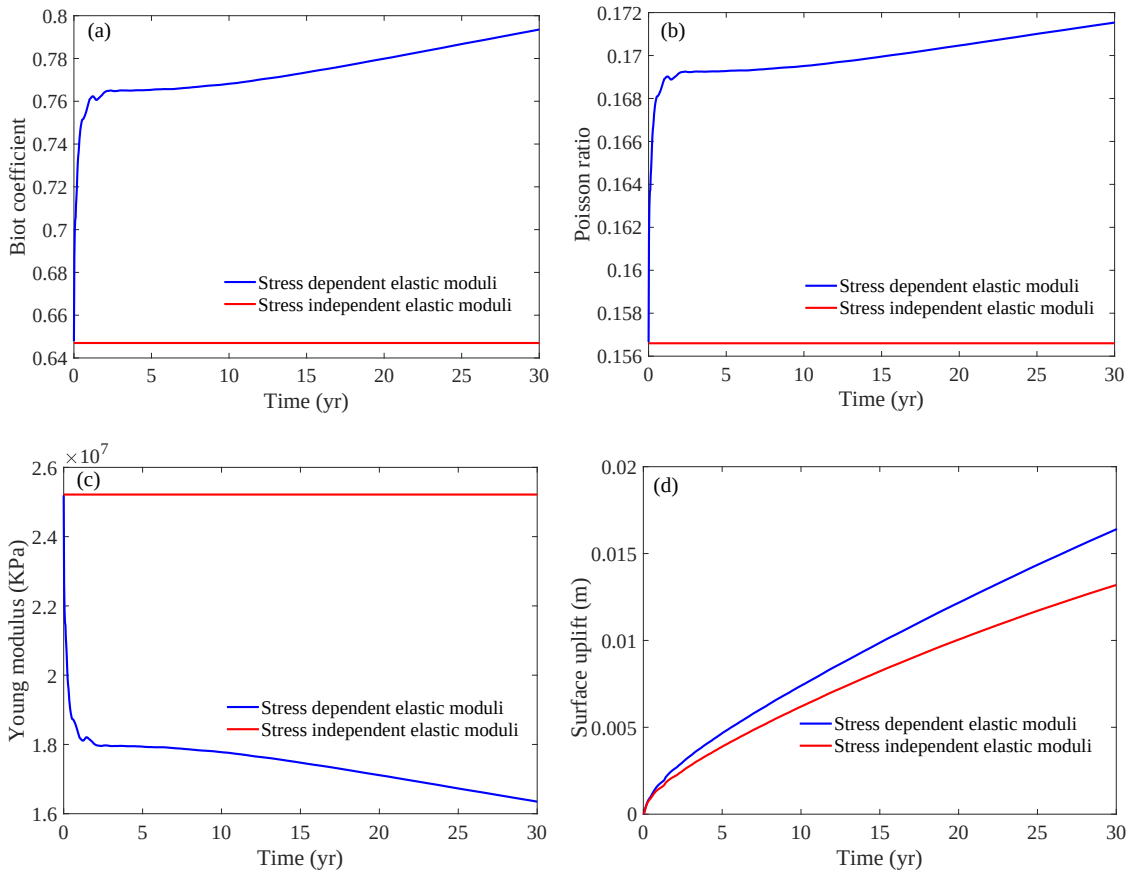

Fig. 4. (a) Biot coefficient changes during injection, (b) Poisson's ratio changes during injection, (c) Young's modulus changes during injection, and (d) surface uplift of the grid block above wellbore.

(1) A scenario which elastic moduli and Biot coefficient are assumed to be constant (2) A scenario which elastic moduli and Biot coefficient are stress dependent. Note that experimental results and derived regression-based equations (Eqs. (2)-(5)) discussed in the previous section provided input data to relate elastic moduli and stress required to perform simulation for Scenario 2.

Note that effective stress in the reservoir decreases due to injection because of pore pressure, and there is a reverse relationship between effective stress and pore pressure. A pore pressure increase from 15.5 to 50 MPa due to fluid injection causes the effective mean stress in the reservoir to decrease from 24 to 9.5 Mpa. Figs. 4(a)-4(c) show the changes in elastic moduli and Biot coefficient during CO_2 injection. Eqs. (2)-(5) were used in the hydromechanical model to estimate changes in elastic parameters and Biot coefficient. Through CO_2 injection, Biot coefficient increases from 0.65 to 0.79, Poisson's ratio increases from 0.158 to 0.171, and Young's modulus decreases from 25 to 16 Gpa. Map views of surface uplift using stress-independent and stress dependent elastic moduli are indicated in Figs. 3(b) and 3(c). Considering stress dependency of elastic moduli leads to a higher uplift specifically above the injection well (16 mm compared to 12.5 mm) after 30 years of injection (Fig. 4(d)). Higher Biot coefficient causes lower effective stress in the reservoir. As a result, a larger portion of pore pressure contributes to poroelastic response to injection. A decrease of Young's modulus causes a softer (more compliant) reservoir, larger reservoir expansion, and higher Earth surface uplift eventually.

As shown in Fig. 4, significant changes are shown in Elastic moduli (Young's modulus and Poisson's ratio) and Biot coefficient at early injection time (as shown in Fig. 4). The changes, however, are less significant during later time (after 2 years of injection). Fig. 5(a) shows the mean effective stress at the wellbore block during the injection period. There is a significant drop in effective stress due to immediate pressure buildup around the wellbore at the early time of CO_2 injection. Such changes in mean effective stress cause significant changes in elastic moduli and Biot coefficient during the early time of CO_2 injection since there is a direct relationship between elastic moduli and effective stress. Fig. 5(c) also shows the changes in mean effective stress away from the wellbore. While change in mean effective stress around the wellbore is more significant at early injection time, mean effective stress shows more uniform trend away from the wellbore. Fig. 5 also shows vertical displacement at a grid around the wellbore and away from the wellbore in the reservoir. The grid vertical displacement follows mean effective stress trend for both scenarios (at the wellbore and away from the wellbore). Note that the combination of all

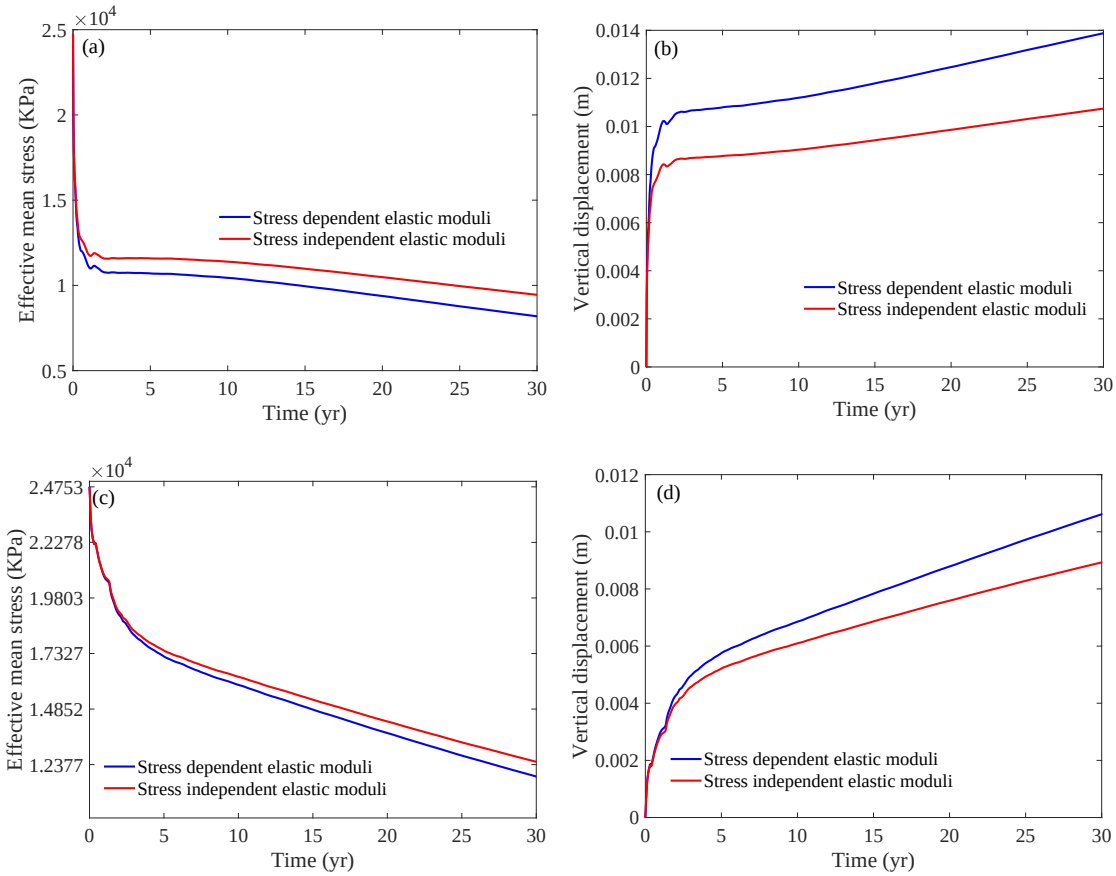

Fig. 5. (a) Effective mean stress at the wellbore grid, (b) vertical displacement at the wellbore grid, (c) effective mean stress away from wellbore grid, and (d) vertical displacement away from wellbore grid.

reservoir blocks displacement (around and away from the wellbore) ultimately causes uplift at the Earth surface (as observed in Fig. 4(d)). Also, elastic moduli of overburden formations affect the transition of vertical displacement from reservoir to the Earth surface.

A porosity of 0.08 and permeability of 10 mD was chosen for modeling purpose in this work to represent Berea geological properties in the Appalachian basin. However, the Berea sandstone geological properties could vary across different basins. One additional scenario was performed to understand the impact of Berea geological properties (specifically higher porosity and permeability) on Earth surface uplift. A porosity of 0.1 and permeability of 20 mD were assigned to the Berea sandstone in the new model. Fig. 6(a) shows the impact of elastic moduli stress dependency on Earth surface uplift in the higher porosity and permeability scenario. Changing permeability and porosity to a higher value would impact injection rate and total mass since wellbore bottom hole pressure is constrained. Cumulative injection mass would be 14.7 million metric tons (7.6×10^9 cubic meters at standard condition) with an average rate of 490,000 metric tons per year in this scenario. Due to pressure increase, effective mean stress decreases and causes changes in elastic moduli during fluid injection and a higher Earth surface uplift compared to the constant elastic moduli scenario (similar to the base case scenario). Note that the pressure front can expand to a larger radius compared to the base scenario due to higher permeability in the model. As a result, the magnitude of surface uplift is higher compared to the base scenario (Fig. 4(d)) after 30 years of injection.

One additional scenario was also performed to understand the impact of injection fluid type (brine instead of CO_2) on Earth surface uplift. Fig. 6(b) shows the impact of elastic moduli stress dependency on Earth surface uplift due to brine injection. Note that the type of injection (brine vs CO_2) causes different injection volume/rate considering wellbore bottom hole pressure is constrained. Cumulative injection mass would be 4 million metric tons (4 million cubic meter at standard condition) with an average rate of 133,000 metric tons per year in this scenario. However, the impact of stress dependency of elastic moduli on the Earth surface uplift would be expected in both cases (CO_2 and brine injection) because the pressure increase occurs due to injection regardless of the type of injected fluid. As a result of pressure increase, effective mean stress decreases which causes changes in elastic moduli during fluid injection and a higher Earth surface uplift compared to the constant elastic moduli scenario. Note that pressure buildup across the reservoir would be less than the base scenario due to the single-phase nature of injection. As a result, the magnitude of surface uplift is lower compared to the base scenario (Fig. 4(d)) after 30 years of injection.

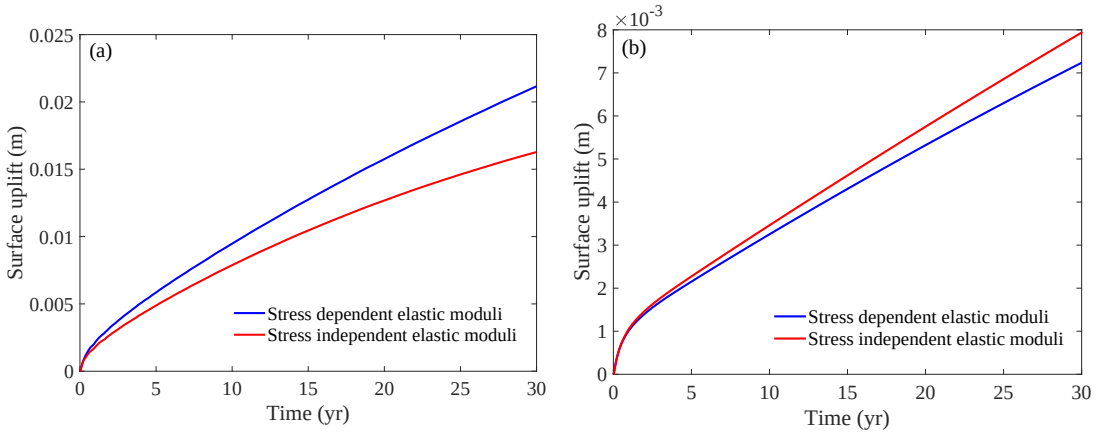

Fig. 6. (a) Surface uplift due to injection in higher porosity and permeability Berea sandstone and (b) surface uplift due to brine injection.

Note that elastic moduli change magnitude determines whether including stress dependency of elastic moduli affects the expected uplift. The change in elastic moduli depends on the type of process (production or injection), effective stress change magnitude, and reservoir rock type. While effective stress decreases due to injection, it increases due to pressure depletion during fluid production. By increasing the effective stress, the elastic moduli and Biot coefficient changes would not be as significant as changes at lower effective stress. On the other hand, decreasing effective stress due to injection causes the elastic moduli and Biot coefficient significant changes (due to the nonlinearity of elastic moduli changes as a result of effective stress change). As a result, the difference between stress independent and stress dependent models to estimate Earth surface deformation would be more pronounced in the injection scenario compared to the production scenario. Changes in elastic moduli would be more considerable if the effective stress decreases significantly. Pressure buildup due to injection in the reservoir determines the effective stress decrease. Such pressure buildup depends on the fluid injection rate as well as the geological properties of the reservoir. Also, the elastic module changes due to effective stress decrease depend on the reservoir rock type. As shown in Fig. 1, elastic moduli in some rock types (e.g., Bentheimer and Berea sandstone) are more sensitive to changes in the effective stress compared to other types (e.g., Indiana limestone).

4. Conclusion

Typically, the hydromechanical models use constant elastic moduli-Biot coefficient to predict geomechanical responses to fluid injection. The effect of stress-dependent elastic moduli on Earth surface uplift during injection is investigated in this study. Laboratory experiments performed in different rock types show that both elastic moduli and Biot coefficient depend on effective stress although the trend would be different for each rock type. Regression-based model was used to relate the effective stress and elastic moduli of Berea sandstone which was imported into the hydromechanical model to capture the impact of elastic moduli stress dependency during the injection.

A hydromechanical model was used to study the effect of stress dependency on the expected uplift. Hydromechanical modeling reveals that surface uplift would be underestimated by neglecting the stress dependency of elastic moduli. A larger uplift would occur by including changes in elastic parameters in the hydromechanical modeling of fluid injection. An increase in Biot coefficient and a decrease in Young's modulus led to an increase in expected uplift. During injection, the effective stress decreases. Due to the non-linear trend between elastic moduli and effective stress, elastic moduli changes would be significant. As a result, the effect of stress dependency on poroelastic response to injection would be significant specifically when the objective of injection is to maximize the pressure and injection volume (decreasing effective stress significantly). Ignoring the stress dependency effect could cause an erroneous estimate of potential surface uplift due to injection. The impact of stress dependency of elastic moduli on surface uplift was observed in modeling scenarios with different injection fluid and reservoir formation with different geological properties.

Acknowledgements

The author would like to thank Mike Heinrichs for providing management review on behalf of Battelle Memorial Institute.

Conflict of interest

The author declares no competing interest.

References

Alvarado, V., Manrique, E. Enhanced oil recovery: An update review. Energies, 2010, 3(9): 1529-1575.

Asghari, K., Dong, M., Shire, J., et al. Development of a

correlation between performance of CO_2 flooding and the past performance of waterflooding in Weyburn oil field. SPE Production & Operations, 2007, 22(2): 260-264.

Biot, M., Willis, D. The elastic coeff cients of the theory of consolidation. Journal of Applied Mechanics, 1957, 24: 594-601.

Bissell, R., Vasco, D., Atbi, M., et al. A full field simulation of the in salah gas production and CO_2 storage project using a coupled geo-mechanical and thermal fluid flow simulator. Energy Procedia, 2011, 4: 3290-3297.

Bjørnarå, T. I., Bohloli, B., Park, J. Field-data analysis and hydromechanical modeling of CO_2 storage at in Salah, Algeria. International Journal of Greenhouse Gas Control, 2018, 79: 61-72.

Blöcher, G., Reinsch, T., Hassanzadegan, A., et al. Direct and indirect laboratory measurements of poroelastic properties of two consolidated sandstones. International Journal of Rock Mechanics and Mining Sciences, 2014, 67: 191-201.

Bohloli, B., Bjørnarå, T. I., Park, J., et al. Can we use surface uplift data for reservoir performance monitoring? A case study from in Salah, Algeria. International Journal of Greenhouse Gas Control, 2018, 76: 200-207.

CMG-GEM. Advance compositional and ghg reservoir simulator user's guide, 2016.

Furre, A.-K., Eiken, O., Alnes, H., et al. 20 years of monitoring CO_2-injection at Sleipner. Energy Procedia, 2017, 114: 3916-3926.

Gale, J. Geological storage of CO_2: What do we know, where are the gaps and what more needs to be done? Energy, 2004, 29(9-10): 1329-1338.

Gambolati, G., Teatini, P. Geomechanics of subsurface water withdrawal and injection. Water Resources Research, 2015, 51(6): 3922-3955.

Gambolati, G., Teatini, P., Baú, D., et al. Importance of poroelastic coupling in dynamically active aquifers of the po river basin, Italy. Water Resources Research, 2000, 36(9): 2443-2459.

Hart, D. J. Laboratory measurements of poroelastic constants and flow parameters and some associated phenomena. Wisconsin, University of Wisconsin-Madison, 2000.

Hart, D. J., Wang, H. F. Variation of unjacketed pore compressibility using gassmann's equation and an overdetermined set of volumetric poroelastic measurements. Geophysics, 2010, 75(1): N9-N18.

Hassanzadegan, A., Guérizec, R., Reinsch, T., et al. Static and dynamic moduli of malm carbonate: A poroelastic correlation. Pure and Applied Geophysics, 2016, 173(8): 2841-2855.

Jha, B., Juanes, R. Coupled multiphase flow and poromechanics: A computational model of pore pressure effects on fault slip and earthquake triggering. Water Resources Research, 2014, 50(5): 3776-3808.

Jun, S., Song, Y., Wang, J., et al. Formation uplift analysis during geological CO_2-storage using the gaussian pressure transient method: Krechba (algeria) validation and south korean case studies. Geoenergy Science and Engineering, 2023, 221: 211404.

Li, C., Laloui, L. Coupled multiphase thermo-hydro-mechanical analysis of supercritical CO_2 injection: Benchmark for the in salah surface uplift problem. International Journal of Greenhouse Gas Control, 2016, 51: 394-408.

Li, H., Zhao, L., Han, D., et al. Experimental study on frequency-dependent elastic properties of weakly consolidated marine sandstone: Effects of partial saturation. Geophysical Prospecting, 2020, 68(9): 2808-2824.

Liu, H., Rutqvist, J. Coupled hydro-mechanical processes associated with multiphase flow in a dual-continuum system: Formulations and an application. Rock Mechanics and Rock Engineering, 2013, 46(5): 1103-1112.

Ma, X., Zoback, M. D. Laboratory experiments simulating poroelastic stress changes associated with depletion and injection in low-porosity sedimentary rocks. Journal of Geophysical Research: Solid Earth, 2017, 122(4): 2478-2503.

Mazzoldi, A., Rinaldi, A. P., Borgia, A., et al. Induced seismicity within geological carbon sequestration projects: Maximum earthquake magnitude and leakage potential from undetected faults. International Journal of Greenhouse Gas Control, 2012, 10: 434-442.

Morris, J. P., Hao, Y., Foxall, W., et al. A study of injection-induced mechanical deformation at the in salah CO_2 storage project. International Journal of Greenhouse Gas Control, 2011, 5(2): 270-280.

Pearse, J., Singhroy, V., Samsonov, S., et al. Anomalous surface heave induced by enhanced oil recovery in northern Alberta: Insar observations and numerical modeling. Journal of Geophysical Research: Solid Earth, 2014, 119(8): 6630-6649.

Pei, L., Blöcher, G., Milsch, H., et al. Thermo-mechanical properties of upper jurassic (malm) carbonate rock under drained conditions. Rock Mechanics and Rock Engineering, 2018, 51(1): 23-45.

Qin, X., Han, D., Zhao, L. Measurement of grain bulk modulus on sandstone samples from the norwegian continental shelf. Journal of Geophysical Research: Solid Earth, 2022, 127(9): e2022JB024550.

Raziperchikolaee, S., Alvarado, V., Yin, S. Effect of hydraulic fracturing on long-term storage of CO_2 in stimulated saline aquifers. Applied Energy, 2013, 102: 1091-1104.

Raziperchikolaee, S., Cotter, Z., Gupta, N. Assessing mechanical response of CO_2 storage into a depleted carbonate reef using a site-scale geomechanical model calibrated with field tests and insar monitoring data. Journal of Natural Gas Science and Engineering, 2021, 86: 103744.

Raziperchikolaee, S., Kelley, M., Gupta, N. A screening framework study to evaluate CO_2 storage performance in single and stacked caprock-reservoir systems of the northern appalachian basin. Greenhouse Gases: Science and Technology, 2019, 9(3): 582-605.

Raziperchikolaee, S., Miller, J. Modeling pressure response into a fractured zone of precambrian basement to understand deep induced-earthquake hypocenters from shallow injection. The Leading Edge, 2015, 34(6): 684-689.

Raziperchikolaee, S., Mishra, S. Statistical based hydrome-

chanical models to estimate poroelastic effects of CO_2 injection into a closed reservoir. Greenhouse Gases: Science and Technology, 2020a, 10(1): 176-195.

Raziperchikolaee, S., Pasumarti, A. The impact of the depth-dependence of in-situ stresses on the effectiveness of stacked caprock reservoir systems for CO_2 storage. Journal of Natural Gas Science and Engineering, 2020b, 79: 103361.

Raziperchikolaee, S., Pasumarti, A., Mishra, S. The effect of natural fractures on CO_2 storage performance and oil recovery from CO_2 and wag injection in an appalachian basin reservoir. Greenhouse Gases: Science and Technology, 2020, 10(5): 1098-1114.

Riley, R., Harper, J., Harrison III, W., et al. Evaluation of CO_2-enhanced oil recovery and sequestration opportunities in oil and gas fields in the MRCSP Region MRCSP Phase II topical report october 2005 october 2010. DOE-NETL Cooperative Agreement DE-FC26-05NT42589, 2010.

Rinaldi, A. P., Rutqvist, J., Finsterle, S., et al. Inverse modeling of ground surface uplift and pressure with ITOUGH-PEST and TOUGH-FLAC: The case of CO_2 injection at in Salah, Algeria. Computers & Geosciences, 2017, 108: 98-109.

Rutqvist, J., Rinaldi, A. P., Cappa, F., et al. Fault activation and induced seismicity in geological carbon storage-lessons learned from recent modeling studies. Journal of Rock Mechanics and Geotechnical Engineering, 2016, 8(6): 789-804.

Sminchak, J. Geologic and hydrologic aspects of brine disposal intervals in the appalachian basingeologic and hydrologic aspects of brine disposal intervals in the appalachian basin. Environmental Geosciences, 2015, 22(4): 97-113.

Song, Y., Jun, S., Na, Y., et al. Geomechanical challenges during geological CO_2 storage: A review. Chemical Engineering Journal, 2023, 456: 140968.

Teatini, P., Gambolati, G., Ferronato, M., et al. Land uplift due to subsurface fluid injection. Journal of Geodynamics, 2011, 51(1): 1-16.

Tran, D., Nghiem, L., Shrivastava, V., et al. Study of geomechanical effects in deep aquifer CO_2 storage. Paper ARMA 10230 Presented at 44th US Rock Mechanics Symposium and 5th US-Canada Rock Mechanics Symposium, Salt Lake City, 27-30 June, 2010.

Tran, D., Settari, A., Nghiem, L. New iterative coupling between a reservoir simulator and a geomechanics module. SPE Journal, 2004, 9(3): 362-369.

Van Genuchten, M. T. A closed-form equation for predicting the hydraulic conductivity of unsaturated soils. Soil Science Society of America Journal, 1980, 44(5): 892-898.

van Wees, J.-D., Pluymaekers, M., Osinga, S., et al. 3-D mechanical analysis of complex reservoirs: A novel mesh-free approach. Geophysical Journal International, 2019, 219(2): 1118-1130.

Verdon, J. P., Kendall, J.-M., Stork, A. L., et al. Comparison of geomechanical deformation induced by megatonne-scale CO_2 storage at Sleipner, Weyburn, and in Salah. Proceedings of the National Academy of Sciences of the United States of America, 2013, 110(30): E2762-E2771.

Verdon, J. P., Stork, A. L. Carbon capture and storage, geomechanics and induced seismic activity. Journal of Rock Mechanics and Geotechnical Engineering, 2016, 8(6): 928-935.

Vidal-Gilbert, S., Tenthorey, E., Dewhurst, D., et al. Geomechanical analysis of the naylor field, Otway Basin, Australia: Implications for CO_2 injection and storage. International Journal of Greenhouse Gas Control, 2010, 4(5): 827-839.

Wang, H. Theory of linear poroelasticity with applications to geomechanics and hydrogeology. New Jersey, USA, Princeton University Press, 2017.

Warpinski, N., Teufel, L. Determination of the effective-stress law for permeability and deformation in low-permeability rocks. SPE Formation Evaluation, 1992, 7(2): 123-131.

Zhang, L., Chen, L., Hu, R., et al. Subsurface multiphase reactive flow in geologic CO_2 storage: Key impact factors and characterization approaches. Advances in Geo-Energy Research, 2022, 6(3): 179-180.

Zhang, L., Nowak, W., Oladyshkin, S., et al. Opportunities and challenges in CO_2 geologic utilization and storage. Advances in Geo-Energy Research, 2023, 8(3): 141-145.

Zheng, W., Kim, J.-W., Ali, S. T., et al. Wastewater leakage in west texas revealed by satellite radar imagery and numerical modeling. Scientific Reports, 2019, 9(1): 14601.